



Impact of tropospheric sulphate aerosols on the terrestrial carbon cycle



Alexey V. Eliseev

A.M. Obukhov Institute of Atmospheric Physics RAS, Moscow, Russia
Kazan Federal University, Kazan, Russia

ARTICLE INFO

Article history:

Received 14 August 2014

Received in revised form 20 October 2014

Accepted 14 November 2014

Available online 25 November 2014

Keywords:

tropospheric sulphates

toxic impact

terrestrial ecosystems

climate projections

ABSTRACT

Tropospheric sulphate aerosols (TSAs) may oxidise the photosynthesising tissues if they are taken up by plants. A parameterisation of this impact of tropospheric sulphate aerosols (TSAs) on the terrestrial gross primary production is suggested. This parameterisation is implemented into the global Earth system model developed at the A.M. Obukhov Institute of the Atmospheric Physics, Russian Academy of Sciences (IAP RAS CM). With this coupled model, the simulations are performed which are forced by common anthropogenic and natural climate forcings based on historical reconstructions followed by the RCP 8.5 scenario. The model response to sulphate aerosol loading is subdivided into the climatic (related to the influence of TSA on the radiative transport in the atmosphere) and ecological (related to the toxic influence of sulphate aerosol on terrestrial plants) impacts. We found that the former basically dominates over the latter on a global scale and modifies the responses of the global vegetation and soil carbon stocks to external forcings by 10%. At a regional scale, however, ecological impact may be as much important as the climatic one.

© 2014 Elsevier B.V. All rights reserved.

1. Introduction

It is broadly accepted now that the atmospheric composition greatly affects the state of the Earth's climate. In turn, the former depends on both natural processes and human activities. In particular, atmospheric aerosols are important for the Earth's climate. Their direct (e.g., related to scattering and absorption of radiation in the solar and near-infrared bands, and change of snow albedo due to deposition of black carbon on snow) and indirect radiative effects (arising because of impact of hygroscopic aerosols on cloud albedo (Twomey, 1974) and cloud lifetime (Albrecht, 1989)) are known to modify climate state both at global and regional scales. Until recently, it was commonly adopted that scattering aerosols dominate in the total aerosol burden, aerosol radiative forcing counteracts the ongoing climate warming and leads to a reduction of precipitation (e.g., Charlson et al., 1992; Mitchell et al., 1995; Taylor and Penner, 1994; Meehl et al., 1996; Lohmann and Feichter, 1997; Boer et al., 2000; Bertrand et al., 2002; Jones et al., 2003a; Volodin and Diansky, 2006; Stendel et al., 2006; Knutson et al., 2006; Meehl et al., 2006; Eliseev et al., 2007). Recent estimates, however, concluded that, despite the central estimate for aerosol direct radiative forcing is negative, its uncertainty range is large and contains both positive and negative values (Myhre et al., 2013).

Nonetheless, one may speculate on other impacts of aerosols on the Earth's climate. First, change in climate state may modify the state of the biogeochemical cycles, hence activating a respective feedback loop. In particular, Jones et al. (2003a) have shown that accounting for the

tropospheric sulphate aerosol in the simulations with the HadCM3L model leads to significant changes in the terrestrial and oceanic carbon uptakes and in the vegetation and soil carbon stocks.

In addition, there is an ecological impact of tropospheric sulphate aerosols (TSAs) which are toxic for terrestrial plants. When these aerosols are taken up by plants, they could oxidise the photosynthetic tissues of these plants. Hence, these aerosols might suppress terrestrial photosynthesis and, therefore, are able to impact the Earth's carbon cycle as well (Semenov et al., 1998; Kuylenstierna et al., 2001). In this respect, the sulphates are similar to the ozone which hurts plant stomata (Sitch et al., 2007). Such an ecological impact of sulphate aerosols was never implemented in global climate models, and its climatic consequences are unknown. Semenov et al. (1998), based on the empirical relations, assessed this impact for Europe and found that it is not significant. However, the TSA ecological impact might be important in other principal aerosol-polluted regions, e.g., China and south-eastern North America. The latter regions also exhibit a relatively high biological productivity. Moreover, plant functional types (PFTs), typical for these regions, exhibit strong sensitivity to toxic impact of sulphate aerosols (Semenov et al., 1998; Kuylenstierna et al., 2001).

We note that sulphate ions enter a number of commonly used agricultural fertilisers (e.g., Huang et al., 2011). Upon entering the soil, sulphate anions may react with soil alkalis and make the soil more fertile. However, if these anions are taken up by plants, they, depending on other conditions, may serve as a nutrient or may still be toxic for these plants (e.g., Rubin, 1985).

In the present paper, a simple representation of the toxic impact of sulphate aerosol on terrestrial gross primary production is suggested. This representation is implemented in the carbon cycle module of the

E-mail address: eliseev@ifaran.ru.

global climate model developed at the A.M. Obukhov Institute of Atmospheric Physics of the Russian Academy of Sciences (IAP RAS CM) (Eliseev and Mokhov, 2011; Mokhov and Eliseev, 2012; Eliseev and Sergeev, 2014). Then, the impact of sulphates on the terrestrial carbon cycle and on the climate–carbon cycle feedback is estimated for simulations covering the last millennium and the future period until the year 2300.

2. Methods

2.1. The model

An implementation of the direct radiative effects of the tropospheric sulphate aerosols in the IAP RAS CM is described by Eliseev et al. (2007). Currently, our model implements only the corresponding direct radiative effect and neglects the respective indirect effects. We acknowledge this caveat of our model.

In addition, the IAP RAS CM accounts for aerosol impact on the fraction of diffuse radiation in the total short-wave radiative flux coming to the upper boundary of the vegetation layer in the model (Eliseev, 2012). Diffuse radiation may penetrate deeper into the canopy and, hence, might amplify gross primary production via enhancement of the photosynthesis of the leaves which are shaded from direct beam (Roderick et al., 2001).

The terrestrial carbon cycle scheme implemented in the IAP RAS CM was validated against the observations collected during the historical period (Eliseev and Mokhov, 2011; Eliseev, 2012; Eliseev and Sergeev, 2014). As a whole, it reproduces the known global and regional features of the terrestrial carbon cycle (gross carbon uptakes and vegetation and soil carbon stocks) with sufficient accuracy. In particular, it simulates the known enhancement of the terrestrial carbon uptake after major volcanic eruptions which emit sulphate aerosols into the stratosphere (Eliseev, 2012). This enhancement in our model is related to the cooling-induced suppression of heterotrophic respiration rather than to the enhancement of the terrestrial primary production by the increased fraction of the diffuse radiation. The latter mechanism is typically adopted for the post-eruption enhancement of terrestrial carbon uptake (Mercado et al., 2009; Volodin et al., 2011; Ciais et al., 2013) based on the measurements by Gu et al. (2003) collected after the Mt. Pinatubo eruption in 1991. However, the relevance of this mechanism for this eruption was questioned by Angert et al. (2004) who simulated the similar uptake without accounting for the enhancement of the terrestrial primary production by diffuse radiation and attributed it to the same mechanism as operating in our model. Some support for their conclusion was found by Krakauer and Randerson (2003) by employing the tree ring data. In addition, Angert et al. (2004) suggested that the measurements reported in (Gu et al., 2003) might be biased because of the neglect of the data obtained in cloudy conditions. In particular, according to (Barford et al., 2001; Law et al., 2002), terrestrial primary production was at minimum rather than at maximum in 1991 in the same place where Gu et al. performed their measurements. In addition Jones et al. (2003b) attributed the post-eruption enhancement of terrestrial carbon uptake to the response of soil respiration rather than to the response of the terrestrial primary production. Finally, some Earth System models, completely neglecting the impact of diffuse radiation on the penetration of the shortwave radiation into the canopy, are able to simulate the post-eruption enhancement of terrestrial carbon uptake (similarly to our model), such as the ECHAM5/JSBACH (Segschneider et al., 2013), the NCAR CSM 1.4 (Frölicher et al., 2013), and a number of Earth System models of intermediate complexity (Foley et al., 2014).

The ecological effects of sulphates on terrestrial gross primary production (GPP) are computed as follows. At the first step, we determine the potential GPP, $f_{GPP,pot}$. Here and below the subscript 'pot' indicates the 'potential' value before accounting for the aerosol stress. Then we

compute this stress, Δf_{GPP} , as an additional term for photosynthesis intensity.

Calculation of the latter term is based on measurements of the change of the biomass of some terrestrial plant species due to their exposure to tropospheric sulphates as a function of the concentration of these sulphates as reported by Semenov et al. (1998). Because in the latter paper the results are figured for the decline of the logarithm of vegetation biomass rather than for the gross primary production, we adapt it to our terrestrial carbon cycle model as follows. First, we assume that carbon stock is a fixed fraction of total biomass for a given PFT. This allows us to relate the coefficients reported by Semenov et al. (1998), b_{sui} thereafter, to living carbon stock instead of total biomass. As a result, sulphate induced suppression of vegetation carbon stock is

$$\Delta c_v = c_{v,pot} \exp(b_{sui}S), \quad (1)$$

where the coefficient b_{sui} is negative and depends on PFT, and S is the near-surface concentration of sulphate aerosols.

Further, we relate Δc_v to the respective changes in gross primary production Δf_{GPP} , autotrophic respiration Δr_v , and litter fall Δf_{fl} . The latter two variables are assumed to depend linearly on vegetation carbon stock:

$$\begin{aligned} \Delta r_v &= k_v \Delta c_v, \\ \Delta f_{fl} &= k_{fl} \Delta c_v. \end{aligned} \quad (2)$$

In turn, gross primary production is assumed to be independent from c_v in the IAP RAS model (Eliseev, 2011; Eliseev and Mokhov, 2011). This leads to

$$\Delta f_{GPP} = (k_v + k_{fl})[1 - \exp(b_{sui}S)]c_v. \quad (3)$$

We caution on a possible interpretation of Eq. (3). First, because the term k_{fl} enters this equation, it may be misinterpreted as saying that the litterfall intensity may affect the gross primary production in our model. Nonetheless, there is no direct influence of the litterfall on the gross primary production. Similarly, sulphates do not directly affect autotrophic respiration and litterfall. Eq. (3) is a consequence of the assumption that the uptake of sulphates by plants depends on biomass, as it follows from Eq. (1). This biomass is affected by litterfall. It is the latter indirect dependence that leads to the term k_{fl} in Eq. (3). We note that Eq. (3) is very similar to that used by Semenov et al. (1998) in their semiempirical model of the TSA impact on vegetation in Europe.

Another thing concerns the term c_v entering Eq. (3). This equation might be misinterpreted as stating that the TSA ecological impact affects the whole biomass rather than the photosynthesising tissues of plants. Again, the term c_v is just a consequence of the usage of Eq. (1). The latter is dictated by the way how the results of the measurements are reported by Semenov et al. (1998). In principle, Eq. (1) may be replaced by a similar equation, but with employment of the carbon stock in these photosynthesising tissues in place of c_v . The latter formulation is likely to be more mechanistic and applicable in a wider set of conditions. In this case, b_{sui} would be recalculated from the values reported by Semenov et al. (1998). However, it would complicate the numerical scheme because some iterative approach should be employed to invert the vegetation carbon budget equation which, contrary to Eq. (2), would become nonlinear.

In addition, as it was already stated, we assume that the carbon stock is a fixed fraction of the total biomass. It means that masses of all chemical constituents, which are present in plants, scale linearly with the vegetation carbon stock. The latter may be invalid generally, but it is consistent with the neglect of interaction between the terrestrial carbon cycle and other biogeochemical cycles in our model. If one considers the latter interaction, it may change the results obtained in the present

paper. Thus, it should be a route for future improvement of the approach suggested in the present paper.

One more point concerns Eq. (2). In particular, because these two equations represent variations of autotrophic respiration and litterfall due to the TSA ecological impact, a more general formulation for them should read

$$\begin{aligned}\Delta r_v &= k_v \Delta c_v + \Delta k_v c_{v,\text{pot}}, \\ \Delta f_{\text{fl}} &= k_{\text{fl}} \Delta c_v + \Delta k_{\text{fl}} c_{v,\text{pot}}.\end{aligned}\quad (4)$$

The terms with Δk_v and Δk_{fl} represent either the response of these fluxes of carbon to climate conditions or the respective response to changes in the amount of nutrients (e.g., Dickinson et al., 2002). However, as it will be shown below, the climate changes associated with the TSA ecological impact are very small and unable to affect markedly the r_v and f_{fl} . In turn, the interactions between the terrestrial carbon cycle and other biogeochemical cycles are neglected in our model. Again, an implementation of such interaction may be the route of improvement of our model.

To finish with the discussion of the assumptions embedded in our model, we remind and highlight that Eq. (3) completely neglects all the fertiliser-related impacts of sulphates (see Section 1).

Values of b_{sul} for each PFT are adapted from the respective central estimates reported by Semenov et al. (1998) (see Table 1). Its magnitude is the largest for cool broadleaf trees and shrubs, somewhat smaller for crops and wetlands, and rather small for grasses. For two plant functional types, warm broadleaf trees and extratropical needleleaf trees, b_{sul} is set equal to zero. For the latter it is done because in Semenov et al. (1998) the results for the impact of sulphates on vegetation carbon stock were statistically insignificant for this PFT. In turn, b_{sul} is zeroed for the former because the just mentioned data set lacks any information on this plant functional type. In this respect, the proposed scheme is conservative. In Section 3.4, we discuss how the results would change if $b_{\text{sul}} \neq 0$ for these two PFTs as well. In the model code, k_v is calculated directly. The calculation for k_{fl} is not so straightforward, however, since litterfall is computed not from the total c_v but from separate carbon stocks for leaves/thin branches and thick branches/hardwood. As a result, we calculate $k_{\text{fl}} = f_{\text{fl}}/c_0$, where $c_0 = \max(c_v, 0.01 \text{ kg C m}^{-2})$. The latter modification is done to avoid numerical problems in grid cells in which the carbon stock is very small. In these grid cell, f_{fl} is very small as well, and such modification affects our results only insignificantly. In addition, it is checked that total gross primary production $f_{\text{GPP}} = f_{\text{GPP,pot}} - \Delta f_{\text{GPP}} \geq 0$. Otherwise, f_{GPP} is zeroed.

The above calculations are done separately in every grid cell and for each PFT.

2.2. Simulations

Our simulation follows the CMIP5 (Coupled Models Intercomparison Project, phase 5) protocol (Taylor et al., 2012). In particular, we have performed ‘historic’ simulation forced by the forcing reconstructions for 850–2005 AD. This simulation is initialised from the model state

occurring after a 200-year spin-up with the forcing values corresponding to the year 850 AD. This simulation was continued until the year 2300 under the Representative Concentration Pathways (RCPs) scenario RCP 8.5 (see Moss et al., 2010). We note, however, that TSA burden remains ‘frozen’ since the year 2100 until the end of the simulation. In our simulations, we employ forcings due to three well-mixed atmospheric greenhouse gases (GHGs, namely, CO_2 , N_2O , and CH_4), tropospheric and stratospheric sulphate aerosols (only direct forcing), change in surface albedo due to land use, and total solar irradiance. Orbital forcing, possible change in vegetation types under climate changes, and changes in ozone burdens in the stratosphere and troposphere are neglected. Ice sheet distribution and heights are prescribed in the model.

We use anthropogenic CO_2 emissions rather than the prescribed concentration of this gas. Carbon dioxide content in the atmosphere is calculated interactively by the model’s carbon cycle module. For other well-mixed GHGs (N_2O and CH_4) atmospheric concentrations are used.

In the CMIP5 historic simulation, the prescribed TSA burden starts to increase in 1850 AD and reaches maximum (1.84 TgS) in the mid-1980s. In scenario RCP 8.5 it decreases to 0.88 TgS in 2100 AD. In addition, the spatial pattern of emissions changes as well. In 1850 AD, almost all sulphates are all over the ocean, with the only exception in North Africa, downwind of the Mediterranean Sea. Then gradually two major regions of pollution develop, one is in Europe, and another is in the south-eastern part of North America. In addition, a secondary pollution region occurs in the southern part of Japan. Pollution in these regions strengthens until the 1980s, and then starts to decay. However, in the 1980s, an additional polluted region in west China develops. The latter starts to dominate in overall sulphate pollution around 2000 AD. In the last decade of the 20th century, pollution in India becomes visible. Aerosol pollution prevails in the latter region until the 2040s. As was already stated, aerosol burden remains constant after 2100 AD. However, to account for the inertia of climate and carbon cycle, we continued our simulations until the year 2300.

We note that the RCP 8.5 scenario is similar to the IS92a scenario used by Jones et al. (2003a) to force their model. So, the results of the present paper may be compared to their results, at least qualitatively.

Four simulations are performed:

- ctrl: the full model is used.
- noGPP: direct impact of sulphate aerosols on terrestrial gross primary production is neglected. Technically, it is achieved by zeroing Δf_{GPP} in Eq. (3).
- SAPI: the preindustrial distribution of atmospheric sulphates during the whole course of the simulation is employed. In the CMIP5 protocol, this preindustrial (PI) distribution corresponds to the year 1850 AD. This suppresses both direct and indirect (arising due to influence of sulphate aerosols on climate) impacts of sulphates. Formally, Δf_{GPP} is not zeroed in these simulations. However, it is almost zero because PI distribution arose due to dimethyl sulphide aerosols (DMS) emitted from the ocean surface and localised basically over oceans. As a result, the difference between noGPP and SAPI simulations may be interpreted as a characteristic of the indirect (climatic) impacts of sulphates on terrestrial carbon cycle.
- ctrl+: In this simulation, b_{sul} for each PFT is set to -10 ppmv^{-1} . This is larger in magnitude than the respective values listed in Table 1. This was done in order to estimate a speculative ‘upper limit’ on direct impact of sulphates on terrestrial carbon cycle. The relevance of this value of b_{sul} for the just mentioned ‘upper limit’ is discussed in Section 3.4. However, we acknowledge that spatial distribution of aerosols, while changes in time, still corresponds to historical evolution of S. Aside from the DMS-affected regions, aerosol burden is largest in the areas of industrial pollution which were mentioned in Section 1. As a result, S is relatively small in tropical forests which are the world’s most productive ecosystem. The approach to assess the parametric sensitivity of the obtained results is conceptually

Table 1

Values of b_{sul} (in ppmv^{-1}) adapted in the IAP RAS CM. Shown are central estimates and the respective standard deviations reported by Semenov et al. (1998).

PFT	Value
Warm broadleaf trees	0
Cool broadleaf trees	-7.2 ± 1.8
Extratropical needleleaf trees	0
C3 grasses	-3.9 ± 0.5
Shrubs	-7.2 ± 2.3
Wetlands	-5.5 ± 2.0
Crops	-6.3 ± 3.0

similar to that used in the papers modelling the oxidising impact of the tropospheric ozone on terrestrial plants (Sitch et al., 2007; Yue and Unger, 2014). In the latter papers, typically two cases are considered (“low ozone sensitivity” and “high ozone sensitivity”) which differ between each other by the values of the coefficients of the prescribed function scaling the gross photosynthesis as a function of plants exposure to ozone.

These simulations are used to isolate different impacts of tropospheric sulphates. In particular, for any variable Y , the climatic impacts of anthropogenic (non-DMS) sulphates may be estimated as a difference

$$\delta_{\text{clim}}Y = Y_{\text{noGPP}} - Y_{\text{SAPI}}. \quad (5)$$

In turn, the respective ecosystem impact reads

$$\delta_{\text{eco}}Y = Y_{\text{ctrl}} - Y_{\text{noGPP}}. \quad (6)$$

Total (climatic + ecosystem) impact, therefore, may be expressed as

$$\delta_{\text{tot}}Y = Y_{\text{ctrl}} - Y_{\text{SAPI}} = \delta_{\text{clim}}Y + \delta_{\text{eco}}Y. \quad (7)$$

The subscripts in the right-hand sides of Eqs. (5)–(7) indicate particular simulations within the above-mentioned set. In addition, we may define $\delta_{\text{eco}+}Y$ and $\delta_{\text{tot}+}Y$, which are similar to $\delta_{\text{eco}}Y$ and $\delta_{\text{tot}}Y$ respectively, but with $Y_{\text{ctrl}+}$ in place of Y_{ctrl} .

We note that our definitions are distinctly different from those used in estimating the impact of aerosols on climate. In particular, thus defined climatic impact, potentially, is a response of the climate and the terrestrial carbon cycle to all radiative effects of sulphates (again, we remind that our model implements only the respective direct effects and completely neglects the indirect ones). In terms of terrestrial carbon cycle, it also accounts for the above-mentioned change in fraction of diffuse radiation in total short-wave radiative flux coming to the upper boundary of the vegetation layer in the model.

Thereafter, only the statistically significant between-simulation differences of variables are shown and discussed. The statistical significance is estimated in terms of the signal-to-noise ratio (SNR) by using a conventional t -criterion. In this paper, only the results with $\text{SNR} > 1$ are presented. We acknowledge that this threshold may be considered as rather small. If we use a larger threshold for SNR (say, 2), the areas in which the results are statistically significant decrease. The latter is not pronounced for the climatic impact of sulphates, but more marked for the respective ecological impact. However, even for the latter, the principal regions in which the TSA ecological impact is statistically significant, e.g., in China and in the southeast of the United States (see below), are still visible but become somewhat disaggregated. As a result, we decided to use the threshold $\text{SNR} > 1$ in our paper for clarity of the presentation.

3. Results

In the following, we will start with the climatic impact of the tropospheric sulphates, and then proceed with the ecological and total impacts. The reason for such a division is the difference in causal chains between climatic and ecological impacts. In the former case, sulphates modify radiative transfer in the atmosphere, affecting climate state and, hence, the state of the carbon cycle. In the latter case, the impact on the carbon cycle is direct, and on the climate state is indirect.

3.1. Climatic impact

Tropospheric sulphates lead to the retardation of greenhouse-induced climate warming (Fig. 1a). This retardation is most pronounced in the middle to subpolar latitudes of the Northern Hemisphere, where the decrease of the annually averaged surface air temperature may be as

large as 1 K in the time of the maximum sulphate burden in the atmosphere (Fig. S1a). The latter is a consequence of the decrease of the short-wave radiation coming to the Earth's surface (Fig. S2a). The simulated aerosol-induced cooling in our model over the land is similar to that simulated by other climate models of different complexity which accounts only for the direct aerosol effect, such as CCCma CGCM1 (Boer et al., 2000), GISS modelE (Hansen et al., 2007), MoBidiC (Bertrand et al., 2002), and CLIMBER-2 (Bauer et al., 2008). Over the oceans, the response in our model is similar to that obtained with the CCCma CGCM1 but markedly smaller than simulated by other just listed models. The reasons for the latter difference are unclear. As a result, the global mean cooling due to aerosol radiative forcing in the IAP RAS CM is smaller than obtained by the four latter models, 0.07 K and 0.2 K, respectively. We note, however, that this discrepancy is partly (but far from completely) caused by the difference in aerosol burden between the simulations employed in the present paper and in the papers published in the 2000s. In particular, anthropogenic sulphate emissions recently revised to be smaller values than it was believed in the 2000s (Smith et al., 2011). In terms of the temperature change since the preindustrial time, TSA retards the climate warming by about 1/4 (Fig. 2a).

Aerosol cooling is comparable between the warm and cold parts of the year. The latter somewhat contradicts the results obtained with the GISS modelE and CLIMBER-2, which both exhibited stronger response to the aerosol loading during warm part of the year. However, at least partly this discrepancy is caused by the neglect of the annual cycle of the TSA burden in our model. In turn, this annual cycle is taken into account in the both just mentioned models.

The underestimation of the annual mean surface air temperature response to the TSA loading into the troposphere over the oceans may lead to the corresponding underestimation of the response of the oceanic carbon uptake. In turn, the underestimation of the respective response over the continents during the warm part of the year may lead to the underestimation of the response in the terrestrial carbon uptake. As a result, one may argue that the climatic impact of tropospheric sulphates on the terrestrial carbon cycle would be even greater than what is obtained in the present paper.

In addition, TSA led to the small reduction of precipitation (Fig. 1b). The largest changes of precipitation occur in the tropics (not shown). Both temperature and precipitation impacts of sulphate aerosols are well known (see Section 1).

Temperature and precipitation changes lead to change in soil moisture. The latter, however, are not so pronounced (Fig. S2a).

As a result, terrestrial gross primary production per unit area, f_{GPP} , is smaller in noGPP than in ctrl over most land regions (Fig. 3a). This occurs despite the increase in the fraction of diffuse radiation η in the total shortwave radiation budget at the upper boundary of the canopy (Fig. S3a). This reflects the larger sensitivity of f_{GPP} in our model to temperature changes and changes of the total flux of photosynthetically active radiation coming to the canopy that occurred since the preindustrial period until the present day than to the respective changes in η . In the late 20th and early 21st centuries, when the loading of sulphates is the largest, this decrease amounts to several tens of $\text{g C m}^{-2} \text{ yr}^{-1}$. The maximum reduction occurs in the polluted regions such as the southeastern part of North America and in Europe, where $\delta_{\text{clim}}f_{\text{GPP}}$ may be $> 100 \text{ g C m}^{-2} \text{ yr}^{-1}$. Here, the aerosol impact is quite substantial, 10–20% of the f_{GPP} change in simulation SAPI during the 20th century. At a global scale, since the last few decades of the 20th century and up to the middle of the 21st century, climate impact of the global terrestrial carbon uptake, $\delta_{\text{clim}}F_{\text{GPP}}$, amounts up to $-2.0 \text{ Pg C yr}^{-1}$ (Fig. 1d), or about 2% of the F_{GPP} change during the 20th century in the simulation SAPI. In terms of the global GPP change since the preindustrial until the first decade of the 21st century, however, the climatic impact of tropospheric sulphates appears to be more important (Fig. 2b). Values of $\delta_{\text{clim}}f_{\text{GPP}}$ basically decay after a few decades after the removal of the sulphate burden from the atmosphere and come close to zero at the end of

the 21st century. However, they are still visible even during the last decade of the 23rd century but with a greatly diminished magnitude (Fig. 3b). The reason for that is a fertilisation of the terrestrial biota by continuously increasing atmospheric CO_2 in our simulations. As a result, the larger F_{GPP} in the simulations is translated to the larger absolute $\delta_{\text{eco}}f_{\text{GPP}}$.

We define the cumulative terrestrial carbon uptake as $U_t = \int_0^t F_t dt$, where F_t is a terrestrial carbon uptake per year, and t is time. The climatic impact of sulphate aerosols decreases the cumulative global terrestrial carbon uptake U_t by up to 11 Pg C in the last decades of the 20th century and in the first decade of the 21st century (Fig. 1d). We do not show the spatial pattern of the cumulative terrestrial carbon uptake because it may be readily inferred from the climatic impact of sulphates on carbon stocks in living vegetation and soil.

Aerosol-induced cooling (via its influence on the CO_2 solubility in sea water) also leads to the enhancement of the oceanic carbon uptake U_o (Fig. 1e), which during the same period may be as large as several Pg C yr^{-1} , or up to 4% of the U_o in the simulation ctrl during the same decades. Similar aerosol-induced decline of the oceanic carbon uptake was noted by Jones et al. (2003a, their Fig. 2) for the years following the eruption of Mt. Pinatubo in 1991.

Taken together, $\delta_{\text{clim}}U_o$ and $\delta_{\text{clim}}U_t$ speed up the growth of the carbon dioxide content in the atmosphere q_{CO_2} by 3 ppmv during the 20th century (Fig. 1f). This amounts a negligibly small part of the q_{CO_2} increase during this century (Fig. 2c).

The negative $\delta_{\text{clim}}f_{\text{GPP}}$ is reflected in the decline of vegetation carbon stock per unit area c_v (Fig. 4a). The latter is the largest in the

regions of the strongest aerosol pollution, and may be as large as several hundreds of $\text{g C m}^{-2} \text{yr}^{-1}$ in the late 20th and early 21st centuries. In relative units, it is up to 20% of c_v change during the 20th century in simulation ctrl. Global vegetation carbon stock C_v is decreased up to 5.6 Pg C in the 1990s due to TSA climatic impact (Fig. 1g), which amounts to several percent of the C_v change during the 20th century in the simulation ctrl (Fig. 2d). We note that our $\delta_{\text{clim}}C_v$ in Fig. 4a is similar to that reported by Jones et al. (2003a, their Fig. 3b) for 1970–2000.

Aerosol-induced decrease of the vegetation carbon stock in the northern mid-latitudes leads to the suppression of litter-fall and, therefore, to the corresponding decrease of soil carbon stock c_s . Around the year 2000, when the tropospheric sulphate burden is near maximum, the latter decrease attains several hundreds of g C m^{-2} , or several percent of the respective c_s value in the simulation ctrl (Fig. 5a). In the northern sub-tropics and in the sub-polar land regions, soil carbon stock slightly increases. This increase is caused by the near-surface cooling, which reduces the decay of organics in soil. This cooling should affect c_s in the mid-latitudes as well, but it is more than compensated by the decreased litter-fall. At the global scale, however, $\delta_{\text{clim}}C_s$, to several percent of the C_s change during the 20th century in simulation ctrl. Our $\delta_{\text{clim}}C_s$ for 2000–2010 is rather dissimilar from the pattern obtained by Jones et al. (2003a, their Fig. 3c) for 1970–2000. We speculate that the reasons for these differences are related to the simulated differences in soil moisture content between our model and the HadCM3L.

Because soil carbon stock is more inertial than the vegetation one, the decay of $\delta_{\text{clim}}C_s$ is retarded with respect to the decay of $\delta_{\text{clim}}C_v$.

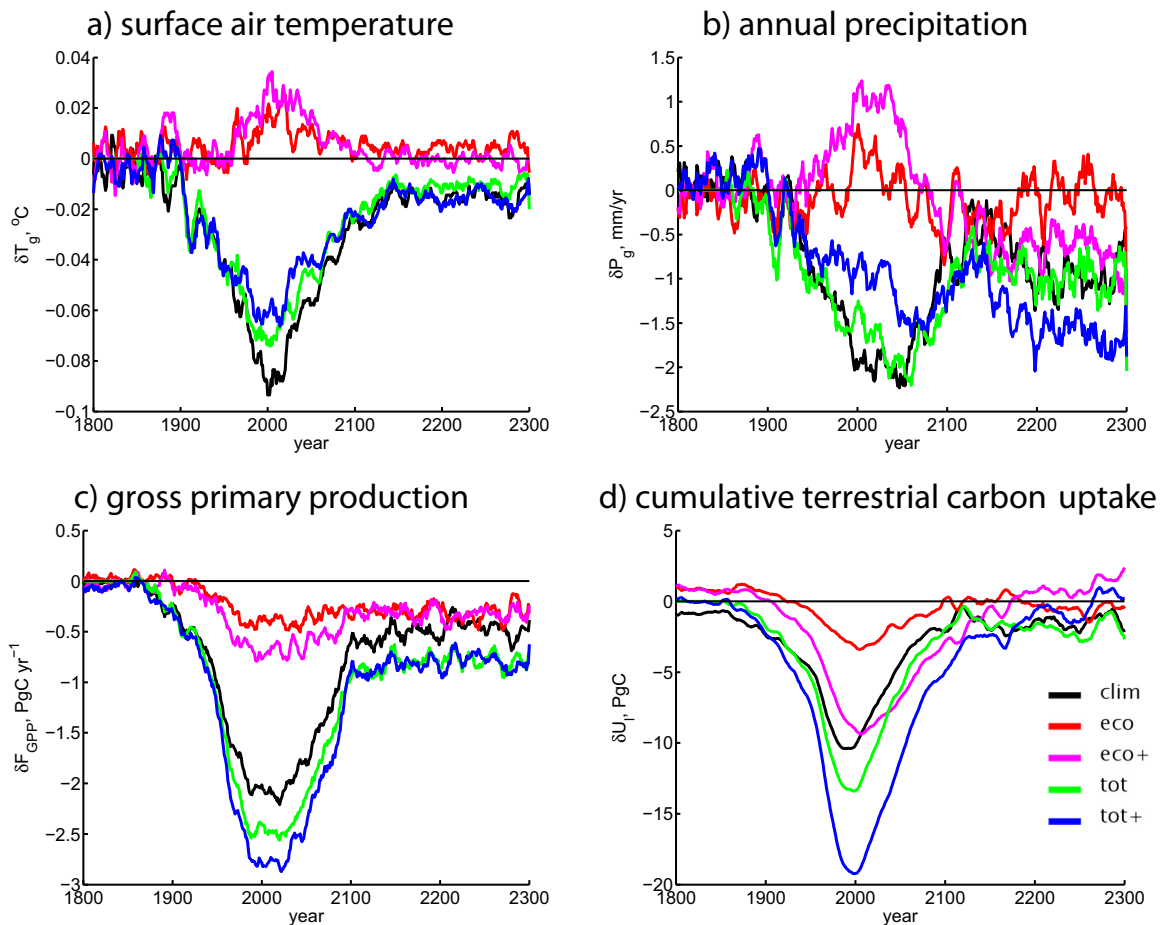


Fig. 1. Time series of differences δ_{clim} , δ_{eco} , $\delta_{\text{eco}+}$, δ_{tot} , and $\delta_{\text{tot}+}$ (see respective definitions in Section 2.2) for globally averaged annual mean surface air temperature (a), annual precipitation (b), total annual terrestrial gross primary production (c), terrestrial and oceanic cumulative uptakes of carbon (d and e correspondingly), CO_2 atmospheric content (f), and vegetation and soil carbon stocks (g and h correspondingly). All values are smoothed by the 11-year running mean.

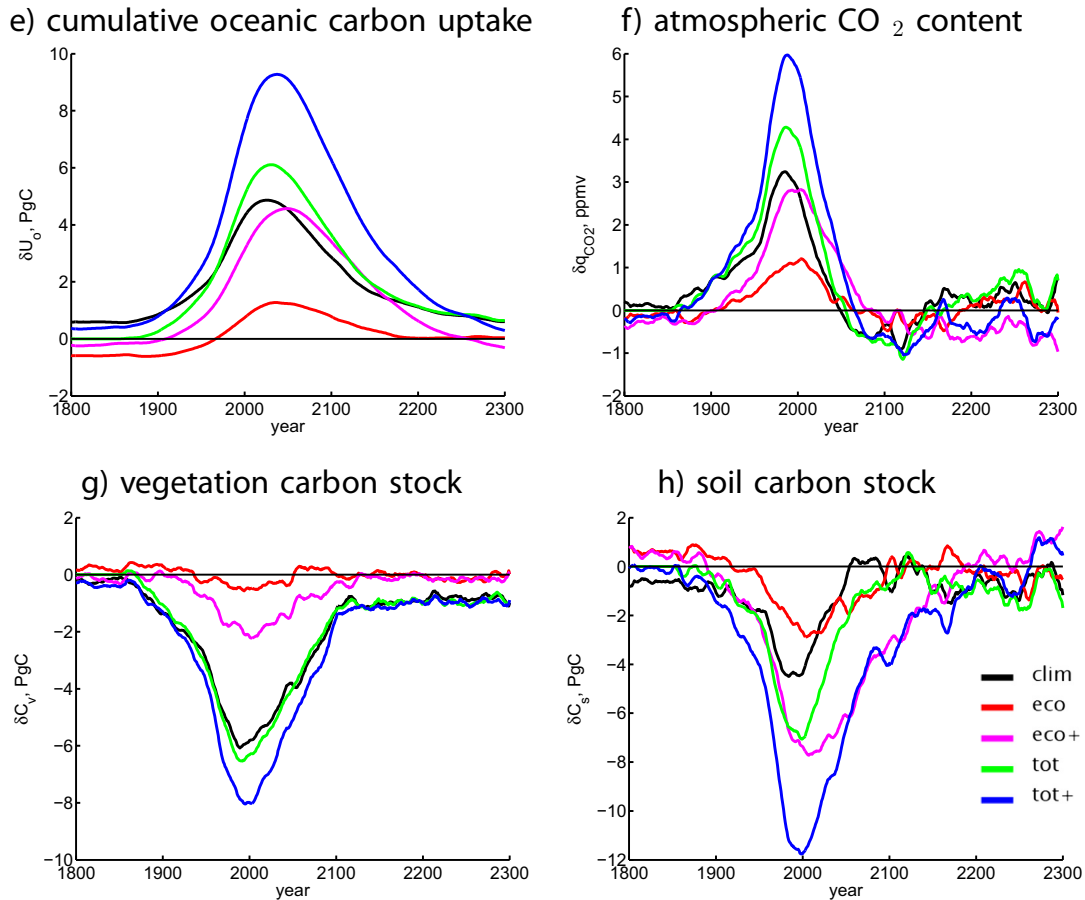


Fig. 1 (continued).

3.2. Ecological impact

Ecological impact of tropospheric sulphates, as a whole, is more modest in comparison to the climatic one. In particular, the changes in the characteristics of climate and the terrestrial carbon cycle since the preindustrial are modified by this impact only to a small amount (Fig. 2a–h). However, the respective regional anomalies of $\delta_{\text{eco}}Y$ for some variables Y may be even larger than the respective $\delta_{\text{clim}}Y$.

For instance, TSA decreases terrestrial gross primary production in the tropics, subtropics, and midlatitudes. As it is expected from the dependence of b_{sui} on PFT, the impact is strongest in the regions where broadleaf trees, shrubs, and crops are abundant. In the late 20th and early 21st centuries, the magnitude of $\delta_{\text{eco}}f_{\text{GPP}}$ is up to several tens of $\text{g C m}^{-2} \text{ yr}^{-1}$ in these regions (Fig. 3c). An unexpected feature, however, is a respective enhancement of f_{GPP} in a few isolated grid cells in the middle and subpolar latitudes. The locations and magnitudes of such isolated patches change somewhat from one decade to another. It occurs because the summers in the late 20th century and the early 21st century in these regions are slightly warmer in simulation ctrl than in simulation noGPP (Fig. S1b). The latter, in turn, is a reflection of the interdecadal variability in our model rather than of a forced signal. We obtain just a negligible ecological impact of tropospheric sulphates on the gross primary production in Europe, which agrees with the semiempirical model results by Semenov et al. (1998).

An important feature of the GPP suppression is that it continues even after the removal of most sulphates from the atmosphere (Fig. 1c). The reason for that is the same as for $\delta_{\text{clim}}f_{\text{GPP}}$: a fertilisation of terrestrial plants by the growing carbon dioxide content in the atmosphere. This fertilisation amplifies the TSA impact during the last two centuries of

our simulations. Moreover, the tropospheric sulphates during the 21st–23rd centuries are localised over areas where the most sensitive to them are PFT abundant. All of these lead to the values of $\delta_{\text{eco}}f_{\text{GPP}}$ which are quite stable since the last decades of the 20th century until the end of the 23rd century (cf. Fig. 3c and d). As a result, the global $\delta_{\text{eco}}f_{\text{GPP}}$ is rather stable as well, about half of Pg C yr^{-1} (Fig. 1c). Around the year 2100 AD it becomes comparable to $\delta_{\text{clim}}f_{\text{GPP}}$.

The overall suppression of the terrestrial gross primary production due to the TSA ecological impact leads to negative $\delta_{\text{eco}}C_v$ in the regions of aerosol pollution (Fig. 4b). In the late 20th century and in the early 21st century the magnitude $\delta_{\text{eco}}C_v$ is of several tens of g C m^{-2} . At a global scale, $\delta_{\text{eco}}C_v$ reaches -0.9 Pg C during these decades (Fig. 1g). Since the mid-21st century, it becomes smaller.

The response of the soil carbon stock to the ecological impact of sulphates is more pronounced than that of the vegetation one. In particular, soil carbon per unit area c_s mostly decreases in the northern middle latitudes (Fig. 5b). The area covered by significant changes of c_s is much larger than that of c_v . Taking also into account that the ecological impact on temperature is rather small as well (Fig. S1b), this more pronounced response of c_s in comparison to c_v is attributed to the larger residence time of carbon in the soil than in the living vegetation. At a global scale, $\delta_{\text{eco}}C_s$ amounts to several Pg C in the last decades of the 20th century and for the first half of the 21st century, which is larger than $\delta_{\text{clim}}C_s$ since the early 21st century. Among the variables, studied in the present paper, soil carbon stock change is the most sensitive to the TSA ecological impact since the preindustrial until the first decade of the 21st century (Fig. 1e). Moreover, the ecologically-induced perturbation decays much slower than the climate-induced one, sustaining at least few Pg C till the end of the 21st century (Fig. 1h).

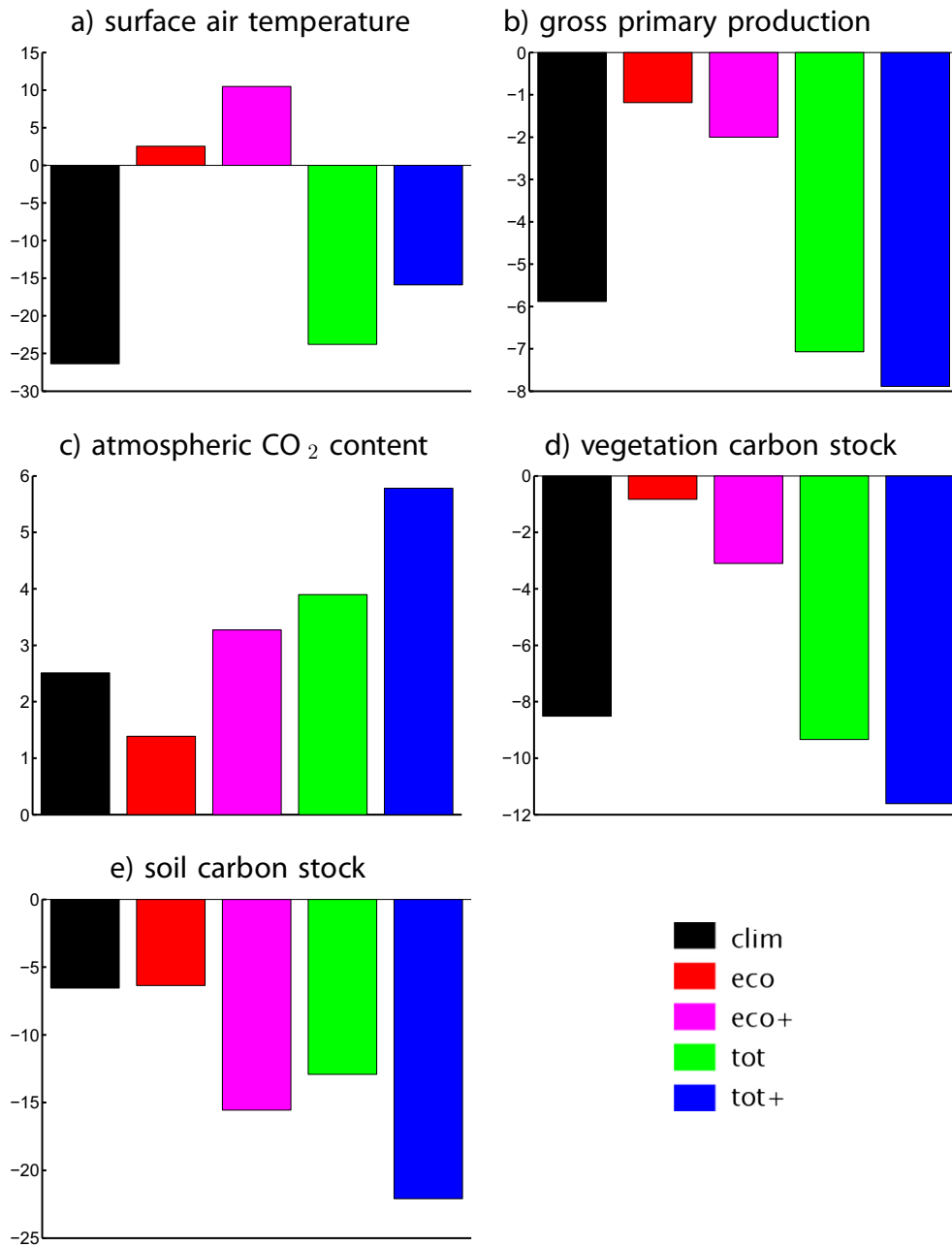


Fig. 2. Relative contribution of the climatic, ecological, and total impacts to changes of the selected variables from 1700–1800 to 2000–2010. Negative (positive) values represent the case when the TSA impact leads to the decrease (increase) of the corresponding variable during the indicated period.

The ecologically-induced change of the cumulative terrestrial carbon uptake is negative (Fig. 1d). It is smaller than the respective climatic impact during the whole simulation. The maximum magnitude of $\delta_{\text{eco}}U_1$ is attained in 1980–2100. During this period, $\delta_{\text{eco}}U_0$ is also near its maximum (Fig. 1e). As a result, the ecological impact of the tropospheric sulphates increases q_{CO_2} during this period by about 1 ppmv.

The associated difference in the globally averaged temperature never exceeds 0.01 K (Fig. 1a). At a regional scale, the ecological impact on surface air temperature and soil moisture is small as well (Figs. S1b and S3b). The same is true for the corresponding impact on the short-wave radiation budget at the canopy upper boundary R_{SWR} and on the fraction of diffuse radiation η in this budget η is small (Figs. S2b and S4b). We note that the climate changes simulated in the present paper as a response to the ecological impact of tropospheric sulphates are

very small and are unable to affect markedly autotrophic respiration of terrestrial plants and litterfall.

In brief, while important for ecosystems at a regional level, the ecological impact of tropospheric sulphates on climate is small at a global scale.

3.3. Total impact

As stated in the previous two sections, the climatic impact of the tropospheric sulphates basically dominates over the respective ecological impact. As a result, for most variables and for most time instants, the total impact is basically determined by the climatic one, at least at a global scale (Fig. 1). However, important exceptions are cumulative terrestrial and oceanic carbon uptakes, and, especially, soil carbon stock. For the latter variable, $\delta_{\text{clim}}C_s$ and $\delta_{\text{eco}}C_s$ equally contribute to $\delta_{\text{tot}}C_s$

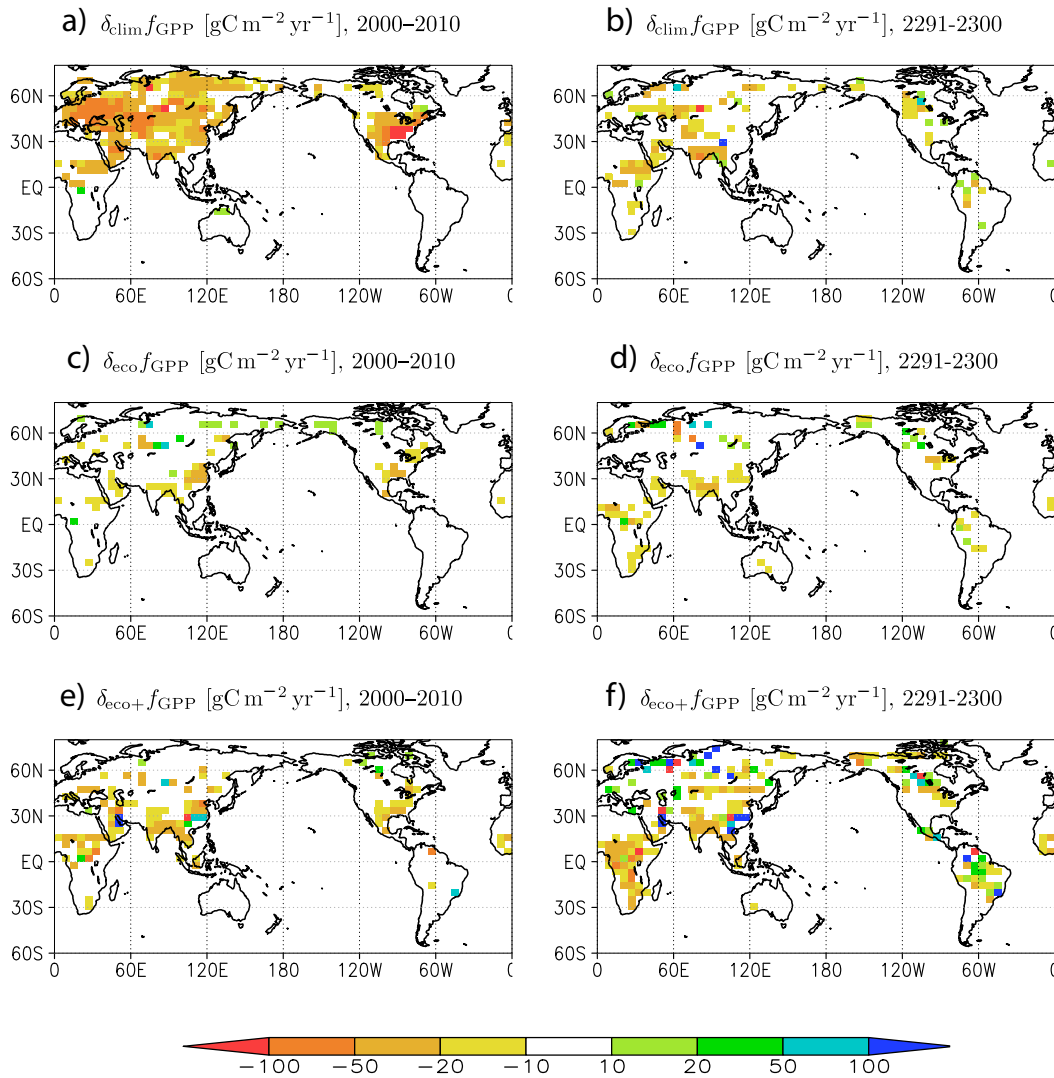


Fig. 3. Spatial distributions of differences δ_{clim} , δ_{eco} , and $\delta_{\text{eco}+}$ for the annual gross primary production per unit area for 2000–2010 and 2291–2300. Only the changes with the signal-to-noise ratio $\text{SNR} > 1$ are shown.

(Fig. 2). Another important exception is the global terrestrial gross primary production in the 22nd and 23rd centuries: $\delta_{\text{tot}}F_{\text{GPP}}$ is roughly and equally split between the corresponding climatic and ecological impacts during these two centuries.

At a regional scale, $\delta_{\text{tot}}Y$ is almost completely determined by the respective $\delta_{\text{clim}}Y$ for surface air temperature, precipitation, and soil moisture content. However, this is generally not true for the ecosystem-related variables. For instance, in some grid cells in the sulphate-polluted regions in the south-eastern parts of Eurasia and North America, the climatic and ecological impacts contribute equally to the response of the gross primary production and vegetation carbon stock to the loading of these aerosols in the troposphere. For soil carbon stock, the values $\delta_{\text{clim}C_s}$ and $\delta_{\text{eco}C_s}$ are generally comparable to each other in most regions of Eurasia and North America.

3.4. Sensitivity of the results to the values of b_{sul}

In this subsection, we discuss the results related to the differences in the simulations ctrl + and noGPP. In the former simulation the magnitudes of b_{sul} are increased to 10 ppbv^{-1} for all plant functional types, including the two ones, for which this coefficient was set to zero in the simulation ctrl.

First of all, we have to discuss the relevance of this value of b_{sul} for the speculative ‘upper limit’ mentioned in Section 2.2. As it was shown in Section 3.2, the TSA ecological impact is most pronounced in the polluted regions such as the south-eastern parts of Eurasia and North America. In our model, these regions are covered mostly by warm broadleaf trees, grasses, and crops. For warm broadleaf trees and crops the value of b_{sul} selected in the simulation ctrl + is slightly above the sum of the central estimate and the respective standard deviation. For grass, it is more than two-fold larger than this sum. However, due to extensive land use in these regions, grasses cover $\leq 5\%$ of these areas. As a result, the value of b_{sul} selected for this simulation is considered as acceptable. Nonetheless, the global results reported below in this section, should be treated with caution because we set b_{sul} to this large value for each PFT, despite the TSA ecological impact is not statistically significant for cool broadleaf trees and unknown for warm trees.

The ecological impact on F_{GPP} is almost doubled in the simulation ctrl + with respect to that in the simulation ctrl, both in terms of the influence on the current state (Fig. 1c) and in terms of the influence on the change since the preindustrial time (Fig. 2b). Partly it is caused by the larger impact in the regions where it was already exhibited in Section 3.2. Here, the ratio $\delta_{\text{eco}+}f_{\text{GPP}}/\delta_{\text{eco}}f_{\text{GPP}}$ scales similarly to the ratio of b_{sul} in the simulations ctrl + and ctrl, respectively (Fig. 3).

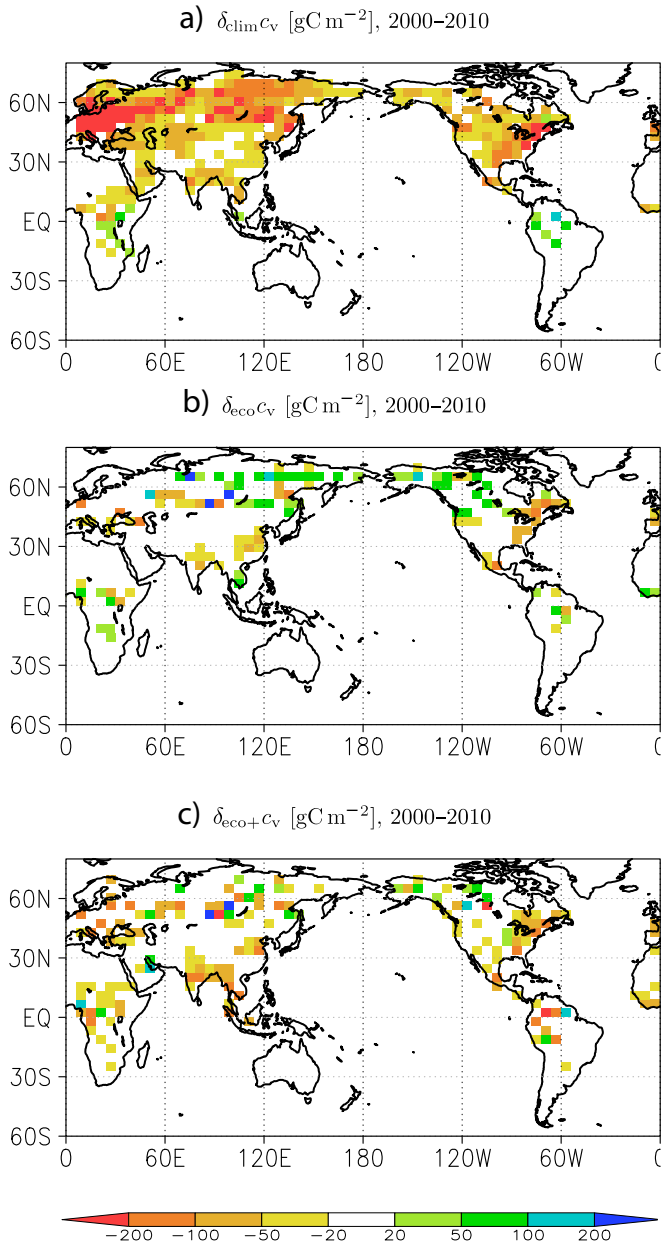


Fig. 4. Spatial distributions of differences δ_{clim} , δ_{eco} , and $\delta_{\text{eco}+}$ for the vegetation carbon stock per unit area for 2000–2010. Only the changes with the signal-to-noise ratio SNR > 1 are shown.

However, an additional, and even more important contribution to $\delta_{\text{eco}+F_{\text{GPP}}}/\delta_{\text{eco}F_{\text{GPP}}}$ is supplied by the TSA ecological impact in the regions which were not affected in the simulation ctrl, such as those covered by extratropical needleleaf forests and, especially, by the tropical forests.

The similar approximately two-fold increase of the ecological impact in the ctrl + simulation with respect to that in the ctrl simulation is found for the oceanic carbon uptake (Fig. 1e) and for the atmospheric CO₂ content (Figs. 1f and 2c). However, the terrestrial carbon uptake is strongly affected than these two variables, and the ratio $\delta_{\text{eco}+f_i}/\delta_{\text{eco}f_i}$ equals almost to four.

The latter leads to $\delta_{\text{eco}+C_v}/\delta_{\text{eco}C_v}$ which is slightly above four (Figs. 1g and 2d). Similar to the gross primary production, the latter is partly due to the stronger response of the vegetation carbon stock in the regions already affected by the ecological impact in the simulation ctrl, and partly due to the response in the regions covered by the tropical forests and extratropical needleleaf forests (Fig. 4c).

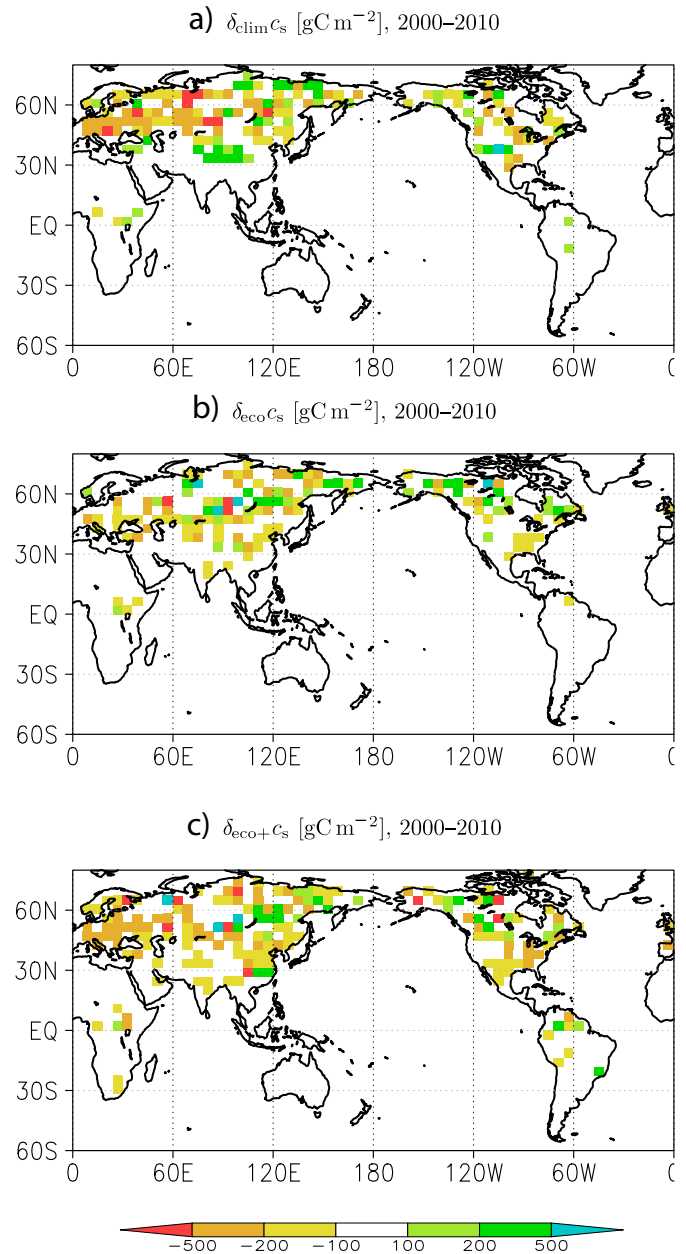


Fig. 5. Similar to Fig. 4 but for the soil carbon stock per unit area.

While $\delta_{\text{eco}+C_s}/\delta_{\text{eco}C_s}$ is close to 2.5 (Figs. 1h and 2e), the spatial pattern of $\delta_{\text{eco}+C_s}$ is qualitatively similar to the pattern of $\delta_{\text{eco}C_s}$ (Fig. 5c). However, the magnitude of the former is larger than that of the latter. This reflects that the climate change rather than the change in litter fall is a primary driver for the C_s change at a multidecadal time scale in our model.

For all variables Y (where Y stands for either gross primary production, or vegetation carbon stock, or soil carbon stock) the larger $\delta_{\text{eco}+Y}$ (relative to $\delta_{\text{eco}Y}$) leads to the larger $\delta_{\text{tot}+Y}$ (relative to $\delta_{\text{tot}Y}$). We did not cite the precise values because they are very uncertain because of the subjective approach to set b_{sul} for the simulation ctrl +. The global values, however, may be read from Figs. 1 and 2.

4. Summary

In this paper, a parameterisation of the impact of tropospheric sulphates on the terrestrial gross primary production is suggested. This parameterisation neglects possible positive effects of sulphates

deposited into the soil with fertilisers. The developed parameterisation is implemented into a global Earth system model. The coupled model is tested in the simulations which are forced by common anthropogenic and natural climate forcings based on historical reconstructions followed by the RCP scenarios.

We found that the climatic (e.g., related to the influence of the tropospheric sulphates on the radiative transport in the atmosphere) impact of sulphate aerosols on the terrestrial carbon cycle is quite substantial. In particular, in the decades of the largest aerosol loading into the atmosphere, the global terrestrial gross primary production is suppressed by 2.0 Pg C yr^{-1} , the global vegetation carbon stock by 6 Pg C , and the global soil carbon stock by 4 Pg C . For vegetation and soil carbon stocks, these values are of the order of 5–10% of the change of the respective variables during the 20th century. At a regional scale, the respective differences are more important. In particular, in the regions, which are most strongly polluted by sulphates, the reduction of the vegetation carbon stock may be as large as 10%. As a result, the buildup of the carbon dioxide in the atmosphere is increased by 3 ppmv . The associated change in globally averaged surface air temperature reaches 0.1 K in the late 20th and in the early 21st centuries.

In turn, the ecological (e.g., related to the toxic influence of sulphate aerosol on terrestrial plants) impact of sulphates is more modest. In particular, even in the decades of the largest aerosol loading, the ecological response of the CO_2 content in the atmosphere never exceeds 1 ppmv , and the associated difference of the globally averaged surface air temperature is smaller than 0.01 K . However, the ecological impact appears important for the terrestrial ecosystems even at a global scale. In particular, the global soil carbon stock reduction may be as large as 4 Pg C at the end of the 20th century and at the beginning of the 21st century. As it was for the climatic impact of sulphates, it is of the order of 5% of the change of the respective variables during the 20th century. The global vegetation carbon stock reduction at a global scale is of the order of 1 Pg C . For the studied variables here, describing the state of ecosystems (terrestrial gross primary production, soil and vegetation carbon stocks) and the ecological impact of sulphates are important at a regional level. In most cases, it roughly doubles the respective climatological impact of sulphates in the troposphere.

We performed the additional simulation in which the coefficient b_{sul} of the photosynthesis suppression by tropospheric sulphates is increased for all plant functional types up to the tentative ‘upper limit’. This ‘upper limit’ is close to the upper limit of the respective values obtained in the field measurements by Semenov et al. (1998). Here, this ‘upper limit’ for b_{sul} is about 1.5 times larger than the respective central estimates. In this additional simulation, the ecological impact of tropospheric sulphates scales with the magnitude of this coefficient in the principal regions where this effect was present already in the standard setup of the model.

The approach to assess the parametric sensitivity of the ecological impact in our paper is similar to that pursued by Sitch et al. (2007) and by Yue and Unger (2014) for the toxic impact of the ozone on terrestrial plants. In this respect, our simulation ctrl is analogous to their ‘low ozone sensitivity’ case, and the simulation ctrl+ might be considered as an analogue for their ‘high ozone sensitivity’ case. In southeast Eurasia, $\delta_{\text{eco}}f_{\text{GPP}}$ ($\delta_{\text{eco}}f_{\text{GPP}}$) which is up to 3% (up to 5%). The respective values in the eastern part of North America are up to 2% (3%). These values may be compared to those due to the toxic impact of O_3 obtained for the latter region by Yue and Unger (2014), which are up to 8% for the ‘low ozone sensitivity’ case, and up to 15% for the ‘high ozone sensitivity’ case. The TSA ecological impact in this region is smaller, but basically of the same order of magnitude. Moreover, Yue and Unger (2014) concluded that the ‘high ozone sensitivity’ case leads to a more realistic performance of their model relative to the benchmark data. We suggest that their simulations might be further improved by considering the ecological impact of tropospheric sulphates as well.

Finally, the present paper is based on a rather limited set of measurements. In particular, these measurements lack any information on very

productive tropical forests. In our additional simulation it was shown that if these forests are sufficiently sensitive to the toxic effect of tropospheric sulphates, it would dramatically enhance the overall TSA impact on the terrestrial carbon cycle. As a result, we highlight an importance of the respective additional measurements unveiling the impact of sulphate aerosols on tropical trees.

Acknowledgement

The author is grateful to G.A. Alexandrov, S. Venevsky and two anonymous referees whose insightful, stimulating, and constructive comments improved the presentation of the obtained results. This work has been supported by the Russian Science Foundation (grant 14-47-00049).

Appendix A. Supplementary data

Supplementary data to this article can be found online at <http://dx.doi.org/10.1016/j.gloplacha.2014.11.005>.

References

- Albrecht, B., 1989. Aerosols, cloud microphysics, and fractional cloudiness. *Science* 245, 1227–1230.
- Angert, A., Biraud, S., Bonfils, C., Fung, I., 2004. CO_2 seasonality indicates origins of post-Pinatubo sink. *Geophys. Res. Lett.* 31 (11), L11103.
- Barford, C., Wofsy, S., Goulden, M., Munger, J., Pyle, E., Urbanski, S., Hutryra, L., Saleska, S., Fitzjarrald, D., Moore, K., 2001. Factors controlling long- and short-term sequestration of atmospheric CO_2 in a mid-latitude forest. *Science* 294 (5547), 1688–1691.
- Bauer, E., Petoukhov, V., Ganopolski, A., Eliseev, A., 2008. Climatic response to anthropogenic sulphate aerosols versus well-mixed greenhouse gases from 1850 to 2000 ad in CLIMBER-2. *Tellus B* 60 (1), 82–97.
- Bertrand, C., Loutre, M.-F., Crucifix, M., Berger, A., 2002. Climate of the last millenium: a sensitivity study. *Tellus* 54A (3), 221–244.
- Boer, G., Flato, G., Reader, M., Ramsden, D., 2000. A transient climate change simulation with greenhouse gas and aerosol forcing: experimental design and comparison with the instrumental record for the twentieth century. *Clim. Dyn.* 16, 405–425.
- Charlson, R., Schwartz, S., Hales, J., Cess, R., Coackley, J., Hansen, J., Hofmann, D., 1992. Climate forcing by anthropogenic aerosols. *Science* 255 (5043), 423–430.
- Ciais, P., Sabine, C., Bala, G., Bopp, L., Brovkin, V., Canadell, J., Chhabra, A., DeFries, R., Galloway, J., Heimann, M., Jones, C., Le Quéré, C., Myneni, R., Piao, S., Thornton, P., 2013. Carbon and other biogeochemical cycles. In: Stocker, T., Qin, D., Plattner, G.-K., Tignor, M., Allen, S., Boschung, J., Nauels, A., Xia, Y., Bex, V., Midgley, P. (Eds.), *Climate Change 2013: The Physical Science Basis. Contribution of Working Group I to the Fifth Assessment Report of the Intergovernmental Panel on Climate Change*. Cambridge University Press, Cambridge and New York, pp. 465–570.
- Dickinson, R., Berry, J., Bonan, G., Collatz, G., Field, C., Fung, I., Goulden, M., Hoffmann, W., Jackson, R., Myneni, R., Sellers, P., Shaikh, M., 2002. Nitrogen controls on climate model evapotranspiration. *J. Clim.* 15 (3), 278–295.
- Eliseev, A., 2011. Estimation of changes in characteristics of the climate and carbon cycle in the 21st century accounting for the uncertainty of terrestrial biota parameter values. *Izv. Atmos. Ocean. Phys.* 47 (2), 131–153.
- Eliseev, A., 2012. Climate change mitigation via sulfate injection to the stratosphere: impact on the global carbon cycle and terrestrial biosphere. *Atmos. Ocean. Opt.* 25 (6), 405–413.
- Eliseev, A., Mokhov, I., 2011. Uncertainty of climate response to natural and anthropogenic forcings due to different land use scenarios. *Adv. Atmos. Sci.* 28 (5), 1215–1232.
- Eliseev, A., Sergeev, D., 2014. Impact of subgrid scale vegetation heterogeneity on the simulation of carbon cycle characteristics. *Izv. Atmos. Ocean. Phys.* 50 (3), 225–235.
- Eliseev, A., Mokhov, I., Karpenko, A., 2007. Influence of direct sulfate-aerosol radiative forcing on the results of numerical experiments with a climate model of intermediate complexity. *Izv. Atmos. Ocean. Phys.* 42 (5), 544–554.
- Foley, A., Willeit, M., Brovkin, V., Feulner, G., Friend, A., 2014. Quantifying the global carbon cycle response to volcanic stratospheric aerosol radiative forcing using Earth System models. *J. Geophys. Res. Atmos.* 119 (1), 101–111.
- Frölicher, T., Joos, F., Raible, C., Sarmiento, J., 2013. Atmospheric CO_2 response to volcanic eruptions: the role of ENSO, season, and variability. *Glob. Biogeochem. Cycles* 27 (1), 239–251.
- Gu, L., Baldocchi, D., Wofsy, S., Munger, J., Michalsky, J., Urbanski, S., Boden, T., 2003. Response of a deciduous forest to the Mount Pinatubo eruption: enhanced photosynthesis. *Science* 299 (5615), 2035–2038.
- Hansen, J., Sato, M., Ruedy, R., Kharecha, P., Lacis, A., Miller, R., Nazarenko, L., Lo, K., Schmidt, G., Russell, G., Aleinov, I., Bauer, S., Baum, E., Cairns, B., Canuto, V., Chandler, M., Cheng, Y., Cohen, A., Del Genio, A., Faluvegi, G., Fleming, E., Friend, A., Hall, T., Jackman, C., Jonas, J., Kelley, M., Kiang, N., Koch, D., Labow, G., Lerner, J., Menon, S., Novakov, T., Oinas, V., Perlwitz, J., Perlwitz, J., Rind, D., Romanou, A., Schmunk, R., Shindell, D., Stone, P., Sun, S., Streets, D., Tausnev, N., Thresher, D., Unger, N., Yao, M., Zhang, S., 2007. Climate simulations for 1880–2003 with GISS modelE. *Clim. Dyn.* 29 (7–8), 661–696.

- Huang, P., Li, Y., Sumner, M. (Eds.), 2011. *Handbook of Soil Sciences: Resource Management and Environmental Impacts*. CRC Press, Boca Raton, Florida.
- Jones, C., Cox, P., Essery, R., Roberts, D., Woodage, M., 2003a. Strong carbon cycle feedbacks in a climate model with interactive CO₂ and sulphate aerosols. *Geophys. Res. Lett.* 30 (9), 1479.
- Jones, C., Cox, P., Huntingford, C., 2003b. Uncertainty in climate–carbon-cycle projections associated with the sensitivity of soil respiration to temperature. *Tellus B* 55 (2), 642–648.
- Knutson, T., Delworth, T., Dixon, K., Held, I., Lu, J., Ramaswamy, V., Schwarzkopf, M., Stenchikov, G., Stouffer, R., 2006. Assessment of twentieth-century regional surface temperature trends using the GFDL CM2 coupled models. *J. Clim.* 19 (9), 1624–1651.
- Krakauer, N., Randerson, J., 2003. Do volcanic eruptions enhance or diminish net primary production? Evidence from tree rings. *Glob. Biogeochem. Cycles* 17 (4), 1118.
- Kuylenstierna, J., Rodhe, H., Cinderby, S., Hicks, K., 2001. Acidification in developing countries: ecosystem sensitivity and the critical load approach on a global scale. *Ambio* 30 (1), 20–28.
- Law, B., Falge, E., Gu, L., Baldocchi, D., Bakwin, P., Berbigier, P., Davis, K., Dolman, A., Falk, M., Fuentes, J., Goldstein, A., Granier, A., Grelle, A., Hollinger, D., Janssens, I., Jarvis, P., Jensen, N., Katul, G., Mahli, Y., Matteucci, G., Meyers, T., Monson, R., Munger, W., Oechel, W., Olson, R., Pilegaard, K., Paw, U.K., Thorgeirsson, H., Valentini, R., Verma, S., Vesala, T., Wilson, K., Wofsy, S., 2002. Environmental controls over carbon dioxide and water vapor exchange of terrestrial vegetation. *Agric. For. Meteorol.* 113 (1–4), 97–120.
- Lohmann, U., Feichter, J., 1997. Impact of sulfate aerosols on albedo and lifetime of clouds: a sensitivity study with the ECHAM GCM. *J. Geophys. Res. Atmos.* 102 (D12), 13685–13700.
- Meehl, G., Washington, W., Erickson, D., Briegleb, B., Jaumann, P., 1996. Climate change from increased CO₂ and direct and indirect effects of sulfate aerosols. *Geophys. Res. Lett.* 23 (25), 3755–3758.
- Meehl, G., Washington, W., Santer, B., Collins, W., Arblaster, J., Hu, A., Lawrence, D., Teng, H., Buja, L., Strand, W., 2006. Climate change projections for the twenty-first century and climate change commitment in the CCSM3. *J. Clim.* 19 (11), 2597–2616.
- Mercado, L., Bellouin, N., Sitch, S., Boucher, O., Huntingford, C., Wild, M., Cox, P., 2009. Impact of changes in diffuse radiation on the global land carbon sink. *Nature* 457 (7241), 1014–1017.
- Mitchell, J., Johns, T., Gregory, J., Tett, S., 1995. Climate response to increasing levels of greenhouse gases and sulphate aerosols. *Nature* 376, 501–504.
- Mokhov, I., Eliseev, A., 2012. Modeling of global climate variations in the 20th–23rd centuries with new RCP scenarios of anthropogenic forcing. *Dokl. Earth Sci.* 443 (2), 532–536.
- Moss, R., Edmonds, J., Hibbard, K., Manning, M., Rose, S., van Vuuren, D., Carter, T., Emori, S., Kainuma, M., Kram, T., Meehl, G., Mitchell, J., Nakicenovic, N., Riahi, K., Smith, S., Stouffer, R., Thomson, A., Weyant, J., Wilbanks, T., 2010. The next generation of scenarios for climate change research and assessment. *Nature* 463 (7282), 747–756.
- Myhre, G., Shindell, D., Bréon, F.-M., Collins, W., Fuglestedt, J., Huang, J., Koch, D., Lamarque, J.-F., Lee, D., Mendoza, B., Nakajima, T., Robock, A., Stephens, G., Takemura, T., Zhang, H., 2013. Anthropogenic and natural radiative forcing. In: Stocker, T., Qin, D., Plattner, G.-K., Tignor, M., Allen, S., Boschung, J., Nauels, A., Xia, Y., Bex, V., Midgley, P. (Eds.), *Climate Change 2013: The Physical Science Basis. Contribution of Working Group I to the Fifth Assessment Report of the Intergovernmental Panel on Climate Change*. Cambridge University Press, Cambridge and New York, pp. 659–740.
- Roderick, M., Farquhar, G., Berry, S., Noble, I., 2001. On the direct effect of clouds and atmospheric particles on the productivity and structure of vegetation. *Oecologia* 129 (1), 21–30.
- Rubin, B., 1985. *A Course on Plant Physiology*. Erevan University, Erevan [in Russian].
- Segschneider, J., Beitsch, A., Timmreck, C., Brovkin, V., Ilyina, T., Jungclaus, J., Lorenz, S., Six, K., Zanchettin, D., 2013. Impact of an extremely large magnitude volcanic eruption on the global climate and carbon cycle estimated from ensemble Earth System model simulations. *Biogeosciences* 10 (2), 669–687.
- Semenov, S., Kounina, I., Koukhta, B., 1998. An ecological analysis of anthropogenic changes in ground-level concentrations of O₃, SO₂, and CO₂ in Europe. *Dokl. Biol. Sci.* 361, 344–347.
- Sitch, S., Cox, P., Collins, W., Huntingford, C., 2007. Indirect radiative forcing of climate change through ozone effects on the land-carbon sink. *Nature* 448 (7155), 791–794.
- Smith, S., van Aardenne, J., Klimont, Z., Andres, R., Volke, A., Delgado Arias, S., 2011. Anthropogenic sulfur dioxide emissions: 1850–2005. *Atmos. Chem. Phys.* 11 (3), 1101–1116.
- Stendel, M., Mogenssen, I., Christensen, J., 2006. Influence of various forcings on global climate in historical times using a coupled atmosphere–ocean general circulation model. *Clim. Dyn.* 26, 1–15.
- Taylor, K., Penner, J., 1994. Climate system response to aerosols and greenhouse gases: a model study. *Nature* 369, 734–737.
- Taylor, K., Stouffer, R., Meehl, G., 2012. An overview of CMIP5 and the experiment design. *Bull. Am. Meteorol. Soc.* 93 (4), 485–498.
- Twomey, S., 1974. Pollution and the planetary albedo. *Atmos. Environ.* 8, 1251–1256.
- Volodin, E., Diansky, N., 2006. Simulation of climate changes in the 20th–2nd centuries with a coupled atmosphere–ocean general circulation model. *Izv. Atmos. Ocean. Phys.* 42 (3), 267–281.
- Volodin, E., Kostrykin, S., Ryaboshapko, A., 2011. Simulation of climate change induced by injection of sulfur compounds into the stratosphere. *Izv. Atmos. Ocean. Phys.* 47 (4), 430–438.
- Yue, X., Unger, N., 2014. Ozone vegetation damage effects on gross primary productivity in the United States. *Atmos. Chem. Phys.* 14 (17), 9137–9153.

Supplementary information to
*Impact of tropospheric sulphate aerosols on
the terrestrial carbon cycle*

A.V. Eliseev

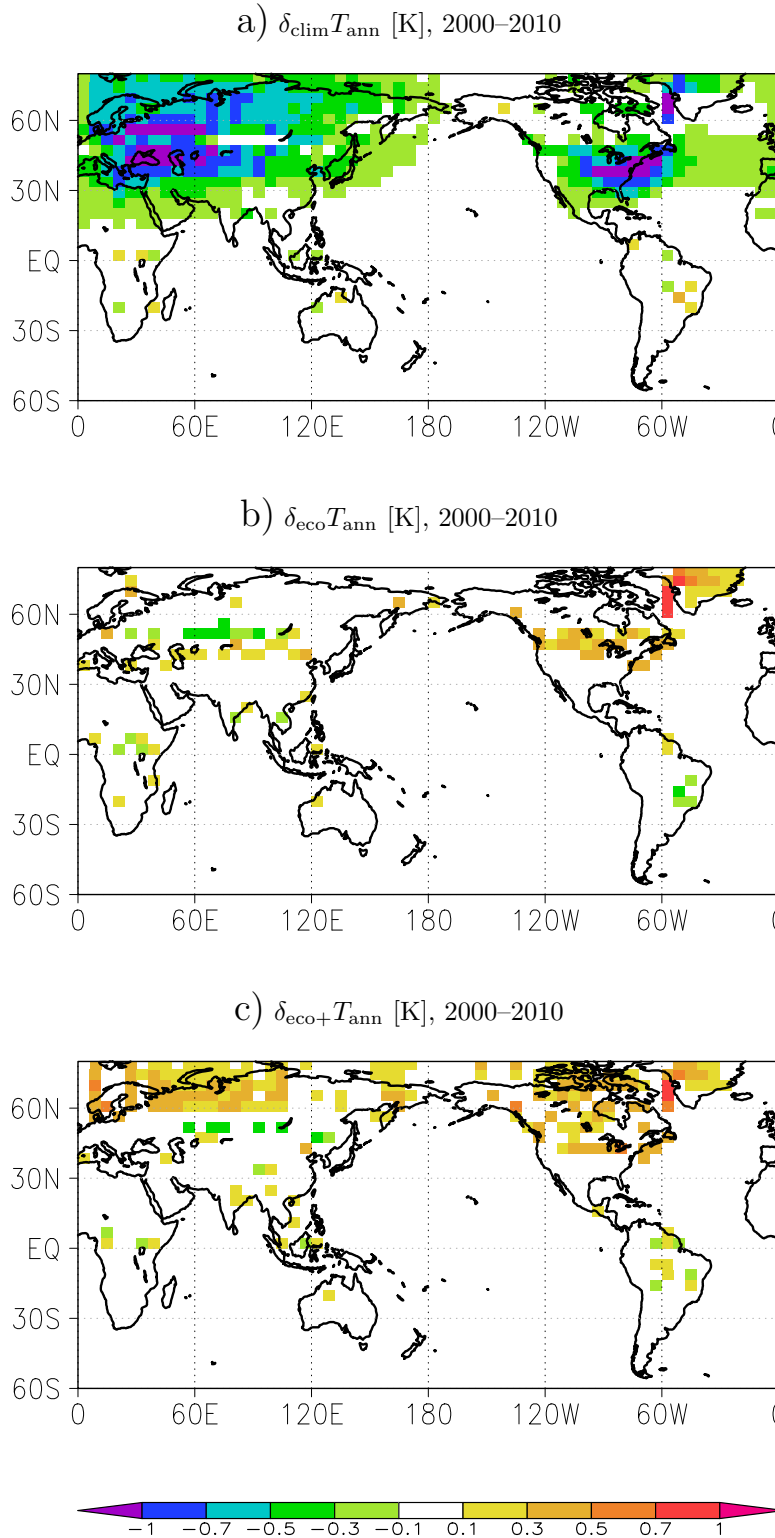
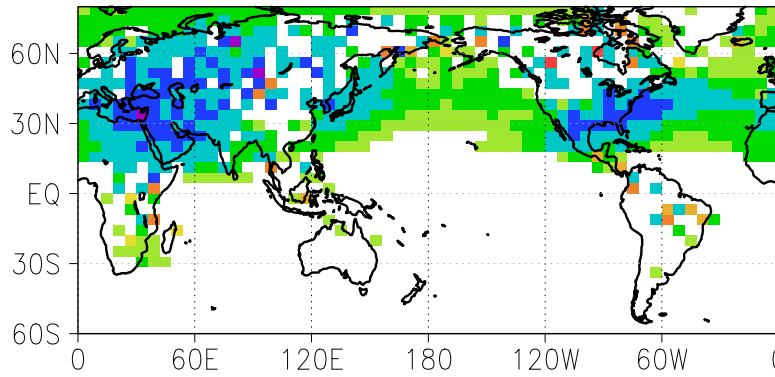
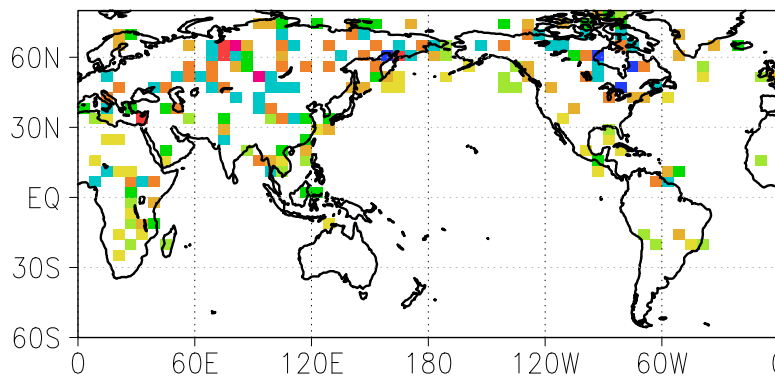


Figure S1: Spatial distributions of differences δ_{clim} , δ_{eco} and $\delta_{\text{eco}+}$ (see respective definitions in Sect. 2.2 of the main text) for the annual mean surface air temperature T_{ann} .

a) $\delta_{\text{clim}} R_{\text{SWR}}$ [W m^{-2}], 2000–2010



b) $\delta_{\text{eco}} R_{\text{SWR}}$ [W m^{-2}], 2000–2010



c) $\delta_{\text{eco+}} R_{\text{SWR}}$ [W m^{-2}], 2000–2010

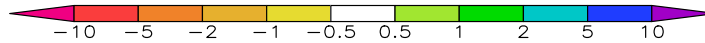
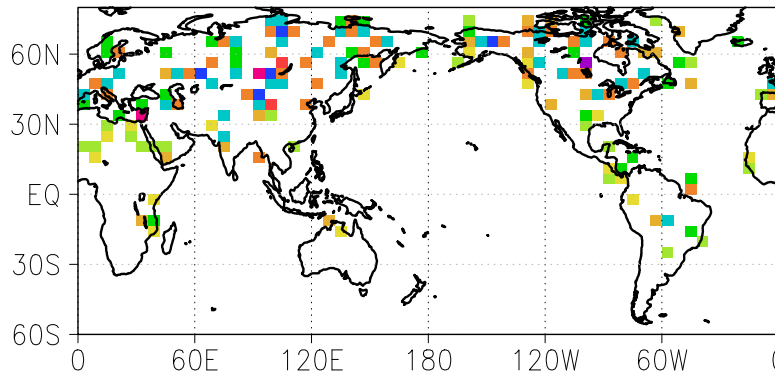


Figure S2: Similar to Fig. S1, but for the budget of the shortwave radiation R_{SWR} at the canopy upper boundary (for bare ground, at the surface; positive downward) in June–August.

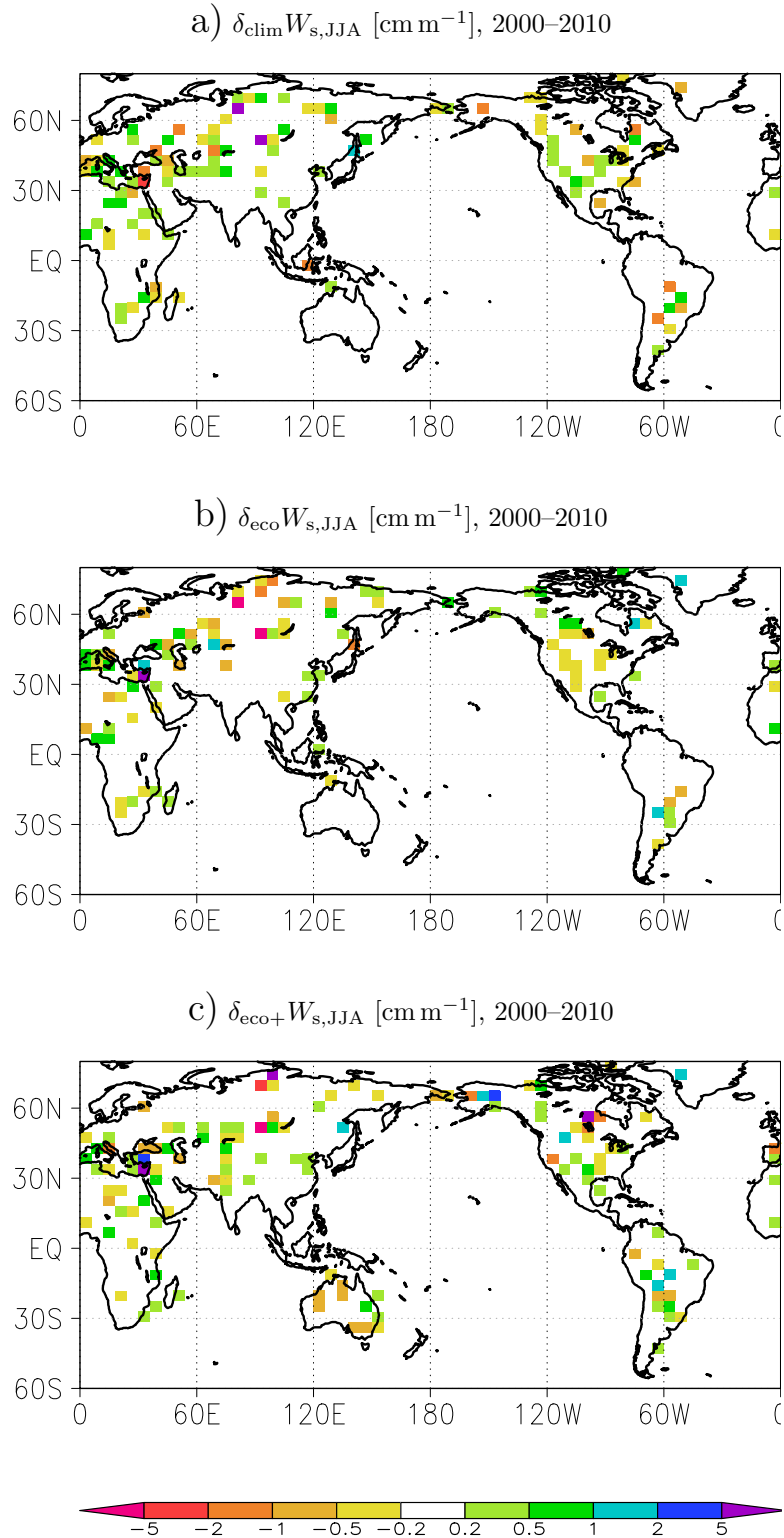


Figure S3: Similar to Fig. S1, but for the moisture content of the upper 5 cm of the soil column in June–August.

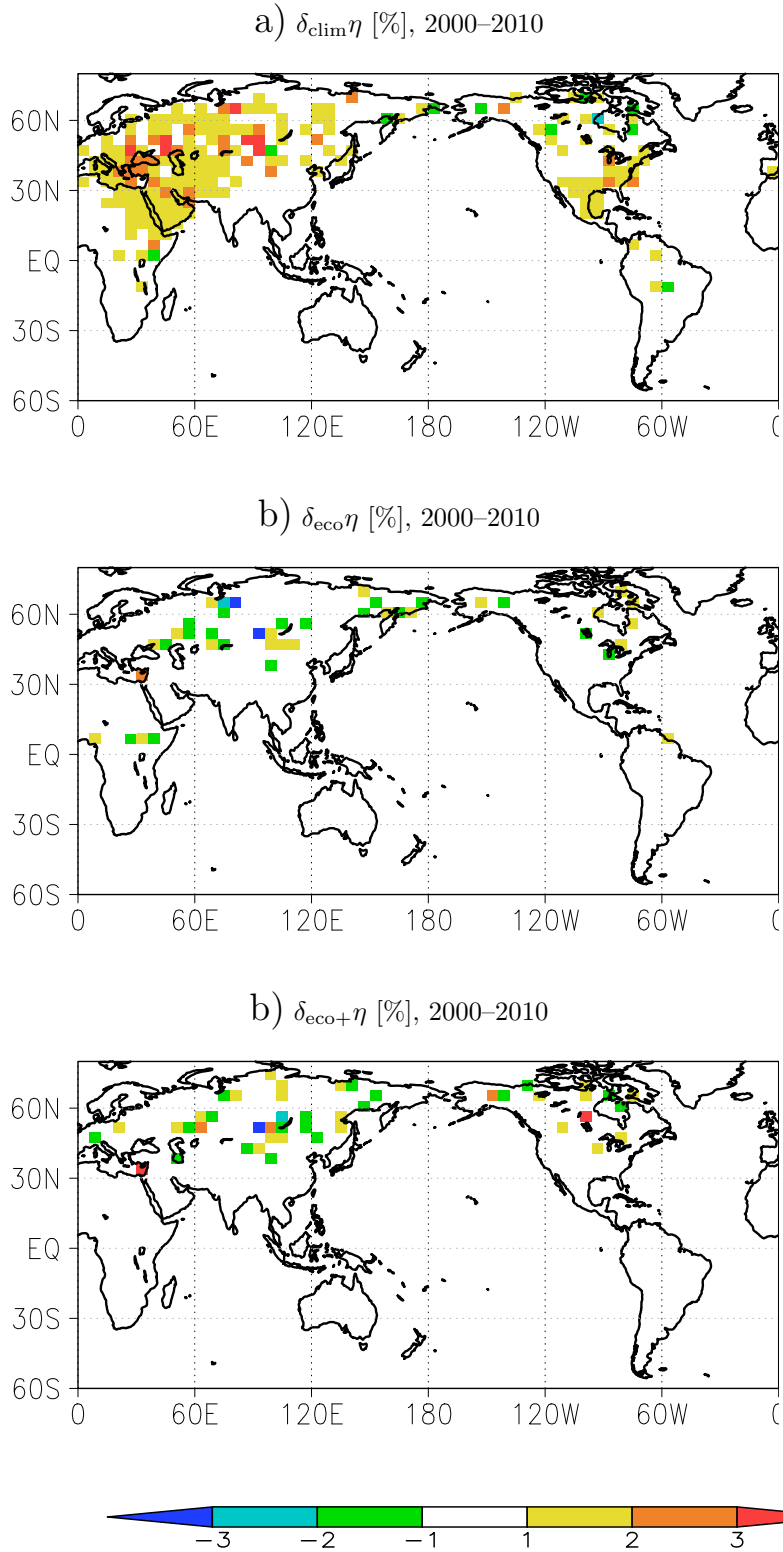


Figure S4: Similar to Fig. S1, but for the fraction of the diffuse radiation η in the total shortwave radiation budget in June–August.